

X-ray interference method for studying interface structures

I. K. Robinson and R. T. Tung
AT&T Bell Laboratories, Murray Hill, New Jersey 07974

R. Feidenhans'l
Risø National Laboratory, DK-4000 Roskilde, Denmark
 (Received 7 April 1988)

We describe a new method of analyzing the structure of the interface between thin films and their substrates. It is based on the interference of the diffraction of the film with the crystal truncation rods of the substrate and yields results of comparable accuracy to Rutherford-backscattering and x-ray standing-wave fluorescence methods. We demonstrate with results for NiSi₂/Si(111).

Crystal-crystal interfaces are two-dimensional (2D) structures which are naturally occurring as grain boundaries and stacking faults in crystals. They are also important in modern materials because of a wide range of interesting properties, including mechanical,¹ electrical,² and magnetic.³ Detailed structural data are an essential first step to understanding these properties and so have attracted much attention. The range of methods available is restricted to techniques that are sufficiently penetrating to reach an interface buried inside a solid, yet sensitive enough to detect a monolayer of atoms there. In thin-film work, effective use has been made of Rutherford-backscattering spectroscopy⁴ (RBS), x-ray standing-wave (XSW) fluorescent yield,^{5,6} and sectional high-resolution transmission electron microscopy⁷ (TEM). X-ray diffraction has been used to deduce interface structure in multilayers⁸ and also to examine superstructures obtained in artificial grain boundaries.⁹ Here, we present a simple x-ray-diffraction technique which reveals the interfacial separation directly, without the requirement of exact modeling of the materials on either side. It makes use of the recent understanding of crystal truncation rods¹⁰ (CTR's), carried over from surface x-ray-diffraction work.

NiSi₂ films grown on Si(111) substrates provide one of the cleanest interfaces known, because of the near perfect lattice match between the crystals. TEM has shown that large areas may be grown completely free from dislocations or interfacial steps.⁷ The preparation involves a high-temperature (500 °C) reaction between a prior deposit of Ni and the substrate itself. The thickness of the deposit is found to control the orientation of the film,⁷ the thinnest films being always "type B" with a reversal of the layer stacking sequence between the overlayer and the substrate, as shown in Fig. 1. Previous studies of interface structure have concentrated on this example because of the ease of preparation and the reproducibility of high-quality films. The ideal interface, with bulk bond lengths throughout and no relaxation, has $d/a_0 = \frac{2}{3}$ assuming $a_1 = a_0$ (Ref. 11). Experimental measurements of the separation by RBS (Ref. 4) have obtained $d/a_0 = 1.106$, and by XSW 1.089 (Ref. 5), or 1.104 (Ref. 6). In each case, a contraction of the interface from its unrelaxed state is ob-

served by amounts 0.06 ± 0.08 Å (Ref. 6), 0.11 ± 0.05 Å (Ref. 5), or 0.06 ± 0.03 Å (Ref. 6). With these results as a reference, we chose to use the type-B NiSi₂/Si(111) interface as a benchmark structure to test our x-ray interference technique.

In deriving the diffracted intensity from the structure shown in Fig. 1, or from an interface structure in general, it is convenient to calculate the contributions from the two crystals separately before adding them together. The interference between them (which depends sensitively upon the interface separation) will arise at that time. Here, for simplicity, we consider only the diffraction along the direction normal to the interface, i.e., the "specular" line, but the results are easily generalized. We assume perfect crystalline order parallel to the interface so that the diffraction is a perfectly sharp line with infinitesimal section. The model is therefore reduced to a one-dimensional

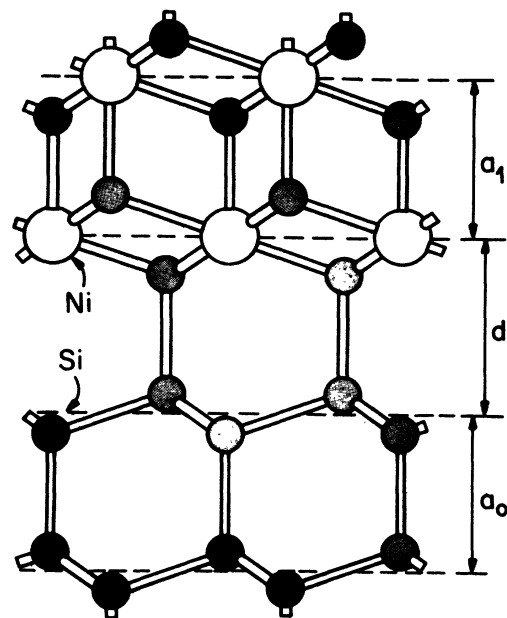


FIG. 1. Schematic "ball and stick" model of a NiSi₂/Si(111) interface, defining the structural parameters a_0 , a_1 , and d .

(1D) sum over layers. Since all layers have the same density of atoms we can use layerwise form factors f_{Si} and f_{Ni} analogous to their atomic counterparts to represent the amplitude of the scattered wave as a fraction of the incident amplitude.¹²

We use the kinematical approximation to add the contributions of the layers; the extent to which this approximation is valid is discussed below. The substrate amplitude, referring to Fig. 1, is a sum over layers for an infinite slab:

$$F_{\text{Si}} = \sum_{n=0}^{\infty} 2f_{\text{Si}} \cos\left(\frac{qa_0}{8}\right) e^{-inqa_0},$$

$$= 2f_{\text{Si}} \cos\left(\frac{qa_0}{8}\right) \frac{1}{1 - e^{-iqa_0}}, \quad (1)$$

where q is the momentum transfer in a diffraction experiment. This is the standard form for the crystal truncation rod¹⁰ for Si(111). The amplitude far from the Bragg peak approaches that of a single layer rather than going to zero. Clearly, this kinematic result is incorrect very close to the Bragg peaks at $q = 2m\pi/a_0$ where F_{Si} becomes infinite. This can be corrected by using a small layerwise absorption term¹⁰ in Eq. (1), or better, by the use of a dynamical treatment: following the Darwin-Prins theory,^{13,14} we arrive at the analogous result for the region close to the Bragg peak:

$$F_{\text{Si}} = \frac{i}{\eta \pm \sqrt{\eta^2 - 1}}, \quad (2)$$

where η is the small deviation from the Bragg condition given by

$$qa_0 = 2m\pi + 2\eta f(q) - 2f(0),$$

$$f(q) = 2f_{\text{Si}} \cos\left(\frac{qa_0}{8}\right).$$

Very close to the Bragg peaks, where $|\eta| \sim 1$, Eq. (2) is better, but elsewhere Eq. (1) is more accurate because of the assumption of a single Bragg peak and other approximations used in deriving Eq. (2).¹³ In the region of interest to the experiment, $|\eta| \gg 1$, yet q is still quite close to a Bragg peak. Either form would be satisfactory, so henceforth, we will choose to consider only the simpler kinematic form of Eq. (1). We note, however, that the kinematic crystal truncation rod of Eq. (1) and the dynamical intensity tails of the Darwin curve of Eq. (2) are just different ways of describing the same thing.

The N -layer thin film can be described in the kinematical limit without approximation. Referring to Fig. 1:

$$F_{\text{NiSi}_2} = \sum_{n=0}^{N-1} \left(f_{\text{Ni}} + 2f_{\text{Si}} \cos\frac{qa_1}{4} \right) e^{inqa_1},$$

$$= \left(f_{\text{Ni}} + 2f_{\text{Si}} \cos\frac{qa_1}{4} \right) \frac{1 - e^{iNqa_1}}{1 - e^{iqa_1}}. \quad (3)$$

This is simply the N -slit function multiplied by the NiSi_2 structure factor.

The magnitudes of the functions given by Eqs. (1) and

(3) are plotted in Fig. 2(a). To the extent that $a_0 \approx a_1$ (Ref. 11) both are symmetric about the Bragg position, $q = 2\pi/a_0$. It is only when the two components are added together with a phase factor corresponding to the interfacial separation that the interference is seen

$$F_{\text{tot}} = F_{\text{Si}} + e^{iqd} F_{\text{NiSi}_2}. \quad (4)$$

The magnitude of Eq. (4) is plotted in Fig. 2(b) for various values of d . Very clearly, there is great sensitivity to this value as it controls the asymmetry between the tails of the Bragg peak.

The point on the curve of greatest sensitivity is when the magnitudes of the two components in Eq. (4) are about equal; this depends upon the number of layers in the film. Near the Bragg peak at $Q = 2\pi/a_0$ letting $q = Q + \Delta q$, $|F_{\text{NiSi}_2}| \approx Nf_{\text{Ni}}$ while $|F_{\text{Si}}| \approx \sqrt{2}f_{\text{Si}}/|\Delta q|a_0$. These are equal when

$$\Delta q = \frac{\sqrt{2}f_{\text{Si}}}{2\pi Nf_{\text{Ni}}} Q. \quad (5)$$

Thus, the interference effects always take place a small fraction (independent of N) of the distance from the Bragg peak to the first node of the film N -slit function [Eq. (3) has nodes at $\Delta q = \pm Q/N$]. For this reason, ex-

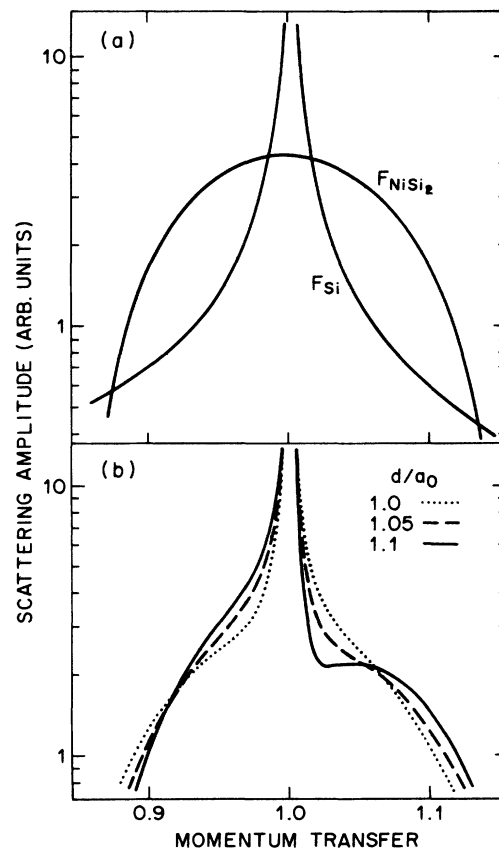


FIG. 2. (a) Scattering amplitudes in the vicinity of the first-order Bragg peak for the Si(111) substrate and NiSi_2 film from Eqs. (1) and (3), respectively. The momentum transfer is in units of $2\pi/a_0$. (b) Total amplitude $|F_{\text{tot}}|^2$ for the sum of the two components given by Eq. (4), as a function of interfacial separation d .

act modeling of the film is unnecessary before useful information about the interface can be obtained.

The Si(111) substrate used in the experiments was cut from a float zone crystal, oriented to within 0.5° of (111) and siton polished. It was prepared by the Shiraki cleaning method¹⁵ and heated to 850°C in ultrahigh vacuum to yield a sharp 7×7 low-energy electron-diffraction (LEED) pattern. 20 Å of Ni were deposited onto the cold substrate from an evaporator, and the sample was heated to 550°C to produce a sharp 1×1 LEED pattern indicating an ordered surface. Finally, 50 Å of amorphous Si were deposited onto the cold sample to prevent oxidation of the silicide film. The thickness was estimated to be 33 Å.

X-ray-diffraction measurements were made with the 4-circle diffractometer on beam line VII-2 at Stanford Synchrotron Radiation Laboratory (SSRL). A pair of Si(111) monochromator crystals were used to select 1.54-Å wavelength x rays from the focused beam. The sample was mounted in air with the center of its face at the intersection of the diffractometer axes. A scintillation detector behind 2 mm (in plane) \times 10 mm (out of plane) slits was used to measure the diffracted beam. Very close to the Bragg peak, the slits were reduced to 1 mm \times 1 mm and the intensity was scaled accordingly. The crystal (111) direction was first brought into the plane of diffraction to an accuracy of 0.1° by means of a goniometer head. Measurements were then made along this direction from (0.7,0.7,0.7) to (1.3,1.3,1.3), as shown in Fig. 3. For each point, a scan of the diffractometer θ angle (axis perpendicular to the scattering plane) was made so that the intensity could be integrated and the background subtracted. This was an important step as the thermal diffuse scattering (TDS) is peaked around the Bragg peak as well but does not form a 1D streak perpendicular to the surface; TDS was therefore suppressed with the background.

Figure 3 also shows the best fit of $|F_{\text{tot}}|^2$ from Eq. (4) to the data. It was found that a superposition of the inten-

sities from a seven-layer region and an eight-layer region (in a 45:55 ratio) fit better than either pure state alone, but this did not have a big impact on the other parameters. It is reasonable to expect a mixture as no attempt had been made to grow a discrete number of layers. The structurally relevant parameters in a four-variable fit to data were

$$d/a_0 = 1.10 \pm 0.02,$$

$$a_1/a_0 = 0.996 + 0.003.$$

As expected, these parameters were only sensitive to the central region of the data, so the relatively poor fit to the side lobes in Fig. 3 is not critical.

The value of d/a_0 shows a contraction of 0.08 ± 0.06 Å from the unrelaxed configuration of the interface, consistent with the other measurements.⁴⁻⁶ The value of a_1/a_0 compares with 0.991 ± 0.001 , obtained by XSW,⁵ using films thicker than ours, and with 0.9925 ± 0.002 for 200-Å films measured by x-ray diffraction.¹⁶ The observed perpendicular mismatch shows an *increasing* trend with film thickness, which is understood to be caused by reversal of the bulk mismatch at the growth temperatures.¹⁶ Thus, these values of a_1/a_0 may not be inconsistent with ours for 25-Å films.

This interference technique allows determination of interfacial structures with comparable accuracy to XSW and RBS. In certain ways, the sensitivity to interfacial separation shown in Fig. 2(b) is reminiscent of the change of phase of the x-ray standing wave across the total reflection region [$|\eta| < 1$ in Eq. (2)] that modulates the fluorescence to report the position of the overlayer atoms. Thus, it is not surprising that the same accuracy is attained; higher accuracy would require use of higher-order Bragg reflections in both cases. There are important differences: the tiny angular range corresponding to $|\eta| < 1$ makes the XSW measurements much harder, and has limited them until recently¹⁷ to samples that are almost perfect single crystals and undistorted by mounting or processing.⁵ The XSW technique has chemical specificity for a unique atom (Ni for example), while all layers contribute in our case, which means that the unit-cell structure of the film must be known. The interference technique, based on the theory of truncation rods,¹⁰ is affected by interfacial roughness or the presence of contaminating layers, whereas the XSW technique is less sensitive to these. Both techniques are acutely sensitive to strain, and measure the "long-range" interface separation from deep inside the bulk of the substrate to the bulk of the film; interfacial strain is therefore integrated into the values of d obtained.

We have demonstrated the method here with a very simple example of a structure with only two parameters. The interference profile is sensitive to the entire interface structure, albeit with a resolution limited by the diffraction order used. For example, if the effects are large enough, it should be possible to quantify the strain fields on either side of the interface, or to reveal disorder and missing layers. Changes in stacking sequence can also be detected if off-axis truncation rods, with a component of parallel momentum transfer, are analyzed as well.¹⁸

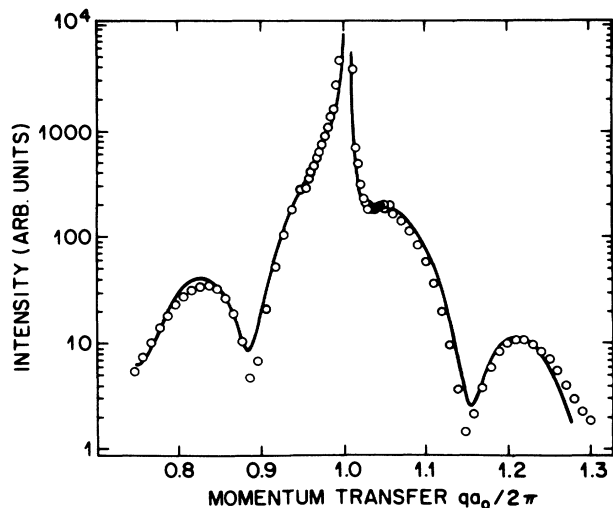


FIG. 3. Integrated intensity of the diffraction along the specular line near the (111) Bragg peak of a $\text{NiSi}_2/\text{Si}(111)$ interface. The fit is to $|F_{\text{tot}}|^2$ from Eq. (4) after optimizing d , a_1 , a scale factor, and the number of layers (see text).

SSRL is supported by the Department of Energy Office of Basic Energy Sciences and the National Institutes of Health Biotechnology Resource Program.

- ¹A. T. Fiory, J. C. Bean, L. C. Feldman, and I. K. Robinson, *J. Appl. Phys.* **56**, 1227 (1984).
- ²R. T. Tung, *Phys. Rev. Lett.* **52**, 461 (1984); J. Tersoff, *ibid.* **52**, 465 (1984).
- ³C. F. Majkrzak *et al.*, *J. Appl. Phys.* (to be published).
- ⁴E. J. van Loenen, J. W. M. Frenken, J. F. van der Veen, and S. Valeri, *Phys. Rev. Lett.* **54**, 827 (1985).
- ⁵E. Vlieg, A. E. M. J. Fischer, J. F. van der Veen, B. N. Dev, and G. Materlik, *Surf. Sci.* **178**, 36 (1986).
- ⁶J. Zegenhagen, K. G. Huang, W. M. Gibson, B. D. Hunt, and L. J. Schowalter (unpublished).
- ⁷R. T. Tung, J. M. Gibson, and J. M. Poate, *Phys. Rev. Lett.* **50**, 429 (1983).
- ⁸D. B. McWhan, in *Synthetic Modulated Structures*, edited by L. L. Chang and B. C. Giessen (Academic, Orlando, 1985).
- ⁹J. Budai, P. D. Bristowe, and S. L. Sass, *Acta Metall.* **31**, 699 (1983).
- ¹⁰I. K. Robinson, *Phys. Rev. B* **33**, 3830 (1986).
- ¹¹The lattice parameters of bulk NiSi₂ (5.406 Å) and Si (5.4307 Å) match to 0.5%. Since the epitaxial film is lattice matched parallel to the interface, the perpendicular mismatch $(a_0 - a_1)/a_0$ should be less than 1.5%.
- ¹²In this paper, the symbols f_{Si} and f_{Ni} refer to the absolute cross section for a layer of atoms. The conversion from the more conventional atomic scattering factor f_e measured in electrons is $f = (n\lambda/\sin\theta)(e^2/mc^2)f_e$ where n is the areal density of atoms, λ the x-ray wavelength, and θ the scattering angle (Ref. 13).
- ¹³R. W. James, *Optical Principles of the Diffraction of X-rays* (Bell and Hyman, London, 1948).
- ¹⁴C. G. Darwin, *Philos. Mag.* **27**, 315 (1914); J. A. Prins, *Z. Phys.* **63**, 477 (1930).
- ¹⁵A. Ishizaka and Y. Shiraki, *J. Electrochem. Soc. Jpn.* **133**, 666 (1986).
- ¹⁶J. Zegenhagen, M. A. Kayed, K. G. Huang, W. M. Gibson, J. C. Phillips, L. J. Schowalter, and B. D. Hunt, *Appl. Phys. A* **44**, 365 (1987).
- ¹⁷D. P. Woodruff, D. L. Seymour, C. F. McConville, C. E. Riley, M. D. Crapper, N. P. Prince, and R. G. Jones, *Phys. Rev. Lett.* **58**, 1460 (1987).
- ¹⁸I. K. Robinson, W. K. Waskiewicz, R. T. Tung, and J. Bohr, *Phys. Rev. Lett.* **57**, 2714 (1986).

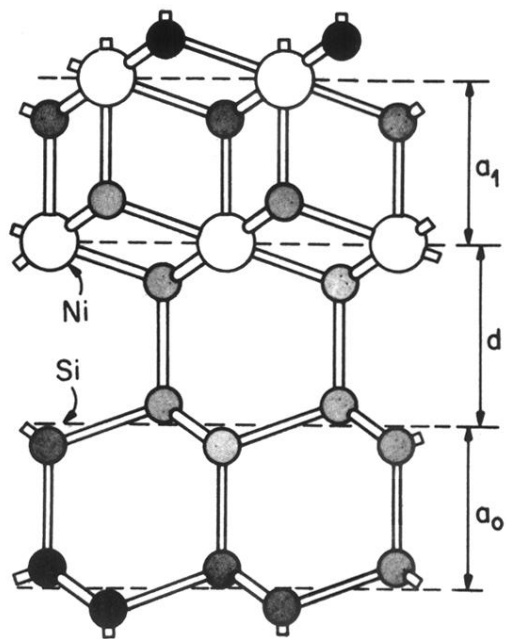


FIG. 1. Schematic “ball and stick” model of a NiSi₂/Si(111) interface, defining the structural parameters a_0 , a_1 , and d .